Parsimonious Model Selection for DTI Tissue Segmentation and Classification: Study on Simulated and Experimental Data

R. Z. Freidlin[1], E. Ozarslan[1], M. E. Komlosh[1], L. C. Chang[1], C. G. Koay[1], D. K. Jones[2], and P. J. Basser[1]

[1]National Institutes of Health, Bethesda, Maryland, United States, [2]University of Cardiff, Cardiff, United Kingdom

ABSTRACT

One aim of this work is to investigate the feasibility of using a hierarchy of models to describe diffusion tensor MRI data. Parsimonious model selection criteria are used to choose among diffusion models having different degrees of symmetry: isotropic, cylindrically symmetric and fully anisotropic. Based on this information, we assess whether we can perform simultaneous tissue segmentation and classification. Both numerical phantoms and diffusion weighted image (DWI) data obtained from excised rat spinal cord are used to test and validate this model selection and clustering framework. Three criteria are used for parsimonious model selection: the *F*-test *t*-test (*F-t*) proposed by Hext, the *F*-test *F*-test (*F-F*) adapted from Snedecor, and the Schwarz Criterion (*SC*). Due to its high sensitivity to the variance estimate and bias in sorting eigenvalues, the *F-F* and *SC* are preferred for segmenting models having cylindrical symmetry.

INTRODUCTION

In this work we examine whether parsimonious model selection criteria applied to a hierarchy of diffusion models can provide simultaneous tissue segmentation and classification based on underlying diffusion properties. A hierarchy of diffusion models and a statistical hypothesis-testing framework were used in the context of the first MR measurement of the translational diffusion tensor to determine whether proton diffusion was isotropic or anisotropic in water and in a skeletal muscle phantom. Subsequently, the possibility of using diffusion models with different degrees of symmetry was proposed to describe diffusion transport in tissue. In this work we test the appropriateness and relative efficiency of four predefined diffusion models: isotropic ($\lambda_1 = \lambda_2 = \lambda_3$), general anisotropic ($\lambda_1 > \lambda_2 > \lambda_3$), and cylindrically symmetric, i.e., prolate ($\lambda_1 > \lambda_2 = \lambda_3$) and oblate ($\lambda_1 = \lambda_2 > \lambda_3$). Three methods for parsimonious model selection used here are based on the *F*-test, *t*-test, and the Schwarz Criterion.

THEORY

First, we estimate all 6 independent elements of the symmetric diffusion tensor, **D**, and the log of the signal, log[*S*(0)], in the absence of the diffusion-weighting, which when written as a vector becomes: $\mathbf{D} = [D_{xx}, D_{yy}, D_{zz}, D_{xy}, D_{xz}, D_{yz}, \log[S(0)]]$. For cylindrically symmetric (oblate and prolate) models the number of free parameters to estimate is reduced from 7 to 5: $[\alpha, \beta, \theta, \varphi, \log[S(0)]]$, where α, β are simple functions of the eigenvalues of **D**, and θ, φ are the spherical coordinates parametrizing the unit eigenvector parallel to the axis of symmetry. For the isotropic model the number of unknown parameters is 2: $[D, \log[S(0)]]$.

The *F*-test in *F-t* hierarchical model selection approach [1] is: $F_{0,iso}^{\text{F-t}} = \dfrac{(SS_T - SS_I)/(fp_T - fp_I)}{(SS_{Sig} - SS_T)/(n - fp_T)}$, where $fp_T = 7$ and $fp_I = 2$ are the numbers of the free parameters in the general anisotropic and isotropic models respectively; n is the number of experimental data points; and SS_{Sig}, SS_T, and SS_I are the total sums of the squares of the acquired signals, and the fitted signals for the anisotropic and isotropic models, respectively. The null hypothesis, that two eigenvalues are equal, can be evaluated using a modification of Hext's *t*-test: $t = (\lambda_i - \lambda_j) \Big/ \sqrt{s^2 (\mathbf{e}_i - \mathbf{e}_j)' (\mathbf{J}'\mathbf{J})^{-1} (\mathbf{e}_i - \mathbf{e}_j)}$ where i =1 and j =2 for the oblate model, i =2 and j =3 for the prolate model, $(\mathbf{J}'\mathbf{J})^{-1}$ is the inverse of the Hessian that approximates the variance/covariance matrix of the estimated parameters, s^2 is the estimate of the residual mean square error on $(n - 7)$ degrees of freedom, and $\mathbf{e}_i$ is the estimated normalized eigenvector associated with the corresponding estimated eigenvalue, λ_i.

In the *F-F* scheme [2], we use an *F*-test for both model selection steps: $F_0^{\text{F-F}} = \dfrac{(RSS_R - RSS_T)/(fp_T - fp_R)}{RSS_R/(n - fp_T - 1)}$ where RSS_R is the residual sum of squares for the reduced model (isotropic: fp_R =2; prolate or oblate: fp_R = 5), and RSS_T is the residual sum of squares for the general anisotropic model ($fp_T = 7$).

The *SC* [3] method imposes a penalty for models with a larger number of free parameters and a larger mean squared residual error. It is defined as: $SC_i = \log(RSS_i/n) + fp_i(\log(n)/n)$

METHODS

The excised rat spinal cord sample was imaged in a 5-mm NMR tube, using a 14.1-T narrow bore magnet with a Bruker Avance imaging console. A diffusion-weighted spin echo pulse sequence was used with TR = 1177 ms, TE = 25 ms, FOV = 4.3×4.3 mm, matrix = 72 × 72 with 300 μm thick slices, NEX=7. Each diffusion-weighted scan was collected with diffusion gradient strength, G = 664 mT/m, corresponding to a b-value of 1250 s/mm^2, applied along 46 different direction. The diffusion gradient pulse duration was δ=1.5 ms, and the gradient separation was Δ = 17.5 ms. The total imaging time was less than 10 hours.

RESULTS

The T2-weighted amplitude image of the excised rat spinal cord is shown in Figure 1. Figures 2 and 3 show consistent assignment of diffusion properties in white and gray matter regions within rat spinal cord.

Fig 1: T2-weighted image.

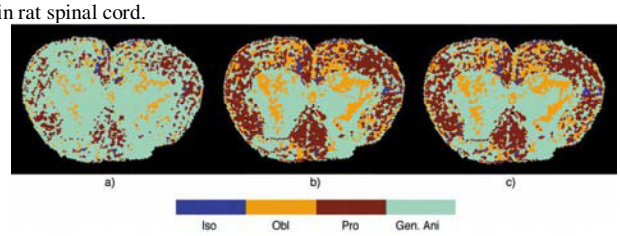

Fig2. Model maps for a) *F-t*; b) *F-F*; c) *SC* approaches

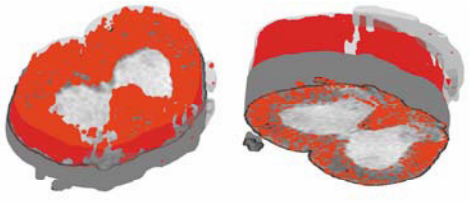

Fig 3: 3D visualization of *F-F* based segmentation

DISCUSSION and CONCLUSION

The maps produced by the proposed parsimonious model selection schemes provide useful information about the underlying tissue microstructure in each voxel. The simplicity and speed of applying *F*- and *t*-tests make these proposed approaches feasible for large DWI data sets routinely encountered in high-resolution microscopic DT-MRI studies or in clinical DT-MRI applications. Results of the phantom simulations increase our confidence in model selection schemes based upon statistical hypothesis tests. When applied to *ex vivo* tissue specimens, where background noise is the primary artifact and other systematic artifacts can be remedied, this approach should work robustly. When using DWI data from living tissue, tests for Gaussianity of the distribution of residuals and for the degree of homoscedasticity must be performed. Our expectation is that these model selection procedures may lead to improved methods of automatic region of interest (ROI) delineation and classification of different tissue types in DT-MRI volume data sets.

BIBLIOGRAPHY: [1] Hext GR. 1963; 50:353–357. [2] Snedecor G, Cochran W. Statistical Methods, 1989. [3] Schwarz G. 1978;6:461–468.